PFC/JA-90-23

CHAOTIC ELECTRON DYNAMICS FOR RELATIVISTIC ELECTRON BEAM PROPAGATION THROUGH A PLANAR-WIGGLER MAGNETIC FIELD

Chiping Chen
Ronald C. Davidson

June, 1990

Plasma Fusion Center
Massachusetts Institute of Technology
Cambridge, MA 02139

Research supported in part by the Department of Energy High Energy Physics Division, the Naval Research Laboratory Plasma Physics Division and the Office of Naval Research.

CHAOTIC ELECTRON DYNAMICS FOR RELATIVISTIC ELECTRON BEAM PROPAGATION THROUGH A PLANAR-WIGGLER MAGNETIC FIELD

Chiping Chen and Ronald C. Davidson
Plasma Fusion Center
Massachusetts Institute of Technology
Cambridge, Massachusetts 02139

ABSTRACT

It is shown that the motion of an individual test electron in a low-density relativistic electron beam propagating through a realizable planar-wiggler magnetic field is nonintegrable and can become chaotic. The chaoticity, which is induced by the transverse spatial inhomogeneities in the wiggler field, poses limits on the wiggler field amplitude and the beam size for beam propagation and free electron laser operation. An approximate condition that determines the onset of chaoticity-induced beam degradation is derived analytically and found to be in good qualitative agreement with the numerical simulations using the Poincaré map.

PACS numbers: 42.55.T, 41.70.+t, 05.45

The free electron laser[1] (FEL) has been an active area of research since the classic experiments by Deacon *et al.*[2] At present, the basic physics of the FEL interaction is well understood for an ideal (constant-amplitude) wiggler field, and coherent radiation has been generated from the visible, to the infrared, to the microwave wavelength range.[3,4] Free electron laser operation often requires sufficiently large gain (growth rate), which increases when the beam current and/or the wiggler field amplitude are increased. In the high-current (high-density) regime and the intense wiggler field regime, the electron motion can be altered significantly by the equilibrium self-field effects[5] associated with the beam space charge and current and by the transverse spatial inhomogeneities in the applied wiggler field. This raises important questions regarding beam transport and the viability of the FEL interaction process in these regimes.

In this rapid communication, we show that the motion of an individual test electron in a low-density relativistic electron beam propagating through a *realizable* planar-wiggler magnetic field (including transverse spatial inhomogeneities) is nonintegrable, and exhibits chaotic behavior when the wiggler amplitude is sufficiently large. Here, chaos[6] refers to the phenomenon in which particle trajectories are sensitive to the initial conditions. In the regime where the chaoticity occurs, it is found that the electrons move back and forth relative to the direction of beam propagation in an unpredictable manner. In addition, it is shown that the threshold value of the wiggler field amplitude for the onset of chaos decreases monotonically as the amplitude of the betatron oscillations in the test electron orbit increases. Therefore, the existence of chaoticity in the electron orbits poses limits on the wiggler field strength and the beam size for beam propagation and FEL operation.

We consider a tenuous electron beam propagating in the z-direction with average axial velocity $V_{zb} = \beta_{zb}c$ through the externally applied magnetic field configuration[7]

$$\vec{B}_w(\vec{x}) = -B_w[\vec{e}_x \cosh(k_w x)\cos(k_w z) - \vec{e}_z \sinh(k_w x)\sin(k_w z)] \ , \tag{1}$$

where $B_w = \text{const.}$ and $k_w = 2\pi/\lambda_w$ are the amplitude and wavenumber, respectively, of the realizable wiggler field. The present analysis assumes that the average cross section of the electron beam extends from $x = -x_b$ to $x = x_b$ in the x-direction, and that the system is uniform the y-direction. Because the electron density and current are assumed to be low, the equilibrium self-electric and self-magnetic fields produced by the beam space charge and current are treated as negligibly small. Therefore, the motion of a typical test electron within the electron beam can be described by the relativistic Hamiltonian

$$H = [(c\vec{P} + e\vec{A}_w)^2 + m^2c^4]^{1/2} = \gamma mc^2 \ . \tag{2}$$

Here, c is the speed of light *in vacuo*; $-e$, m, and γ are the electron charge, rest mass, and relativistic mass factor, respectively; the canonical momentum $\vec{P}$ is related to the mechanical momentum $\vec{p}$ by $\vec{P} = \vec{p} - (e/c)\vec{A}_w(\vec{x})$; and

$$\vec{A}_w(\vec{x}) = \frac{mc^2 a_w}{e}\cosh(k_w x)\sin(k_w z)\vec{e}_y \tag{3}$$

is the vector potential for the wiggler magnetic field $\vec{B}_w(\vec{x}) = \nabla \times \vec{A}_w(\vec{x})$. In Eq. (3), $a_w = eB_w/mc^2k_w$ =const. is the usual dimensionless wiggler amplitude. It is readily shown from Eq. (3) that the wiggler magnetic field satisfies the vacuum Maxwell equation $\nabla \times B_w(\vec{x}) = 0$. Because the Hamiltonian in Eq. (2) is independent of time t and coordinate y, it follows that the total electron energy, $H = \gamma mc^2$, and the y-component of canonical momentum, $P_y = p_y - eA_{yw}(x,z)/c$, are exact constants of the motion in the limit of a tenuous electron beam. Substituting Eq. (3) into Eq. (2) and assuming that $P_y = 0$ readily yields

$$H = [c^2P_x^2 + c^2P_z^2 + a_w^2m^2c^4\cosh^2(k_wx)\sin^2(k_wz) + m^2c^4]^{1/2} = \text{const.} \qquad (4)$$

The Hamiltonian in Eq. (4) describes the electron motion in the three-dimensional phase space (z, P_x, P_z) because x can be determined from the condition $H = \text{const}$. In addition, the phase space is periodic in z with the periodicity $\pi/k_w = \lambda_w/2$, and invariant under the canonical transformations $(x, P_x) \rightarrow (-x, -P_x)$ and $(y, P_y) \rightarrow (-y, -P_y)$.

For the electrons at the beam center ($x = 0$), the factor $\cosh^2(k_wx)$ in Eq. (4) is equal to unity, and the x-component of canonical momentum, $P_x = p_x$, is a constant of the motion. Therefore, for $P_x = 0$, the Hamiltonian in Eq. (4) reduces to a pendulum-like Hamiltonian of the form $\hat{H}(z, P_z) = [c^2P_z^2 + a_w^2m^2c^4\sin^2(k_wz) + m^2c^4]^{1/2}$, which is integrable. As far as free electron laser applications are concerned, we are interested here in the untrapped orbits, which correspond to constant-energy contours with energy $\hat{H} > (1+a_w^2)^{1/2}mc^2$ in the phase space (z, P_z). Electrons displaced from the beam center undergo the so-called betatron oscillations in addition to the wiggle motion induced by the transverse wiggler field. It is well known for $a_w \ll \gamma_b$ that the motion of an individual electron is regular and can be described by a superposition of the (fast) wiggle motion and the (slow) betatron oscillations induced by the transverse spatial inhomogeneities in the wiggler field.[7] That is, the electron wiggles in the y-direction at frequency $ck_w\beta_{zb}$ and oscillates in the x-direction at the betatron frequency $\omega_\beta = ck_wa_w/\sqrt{2}\gamma_b$, while traveling axially with average axial velocity $\beta_{zb}c$. Here, $\beta_{zb} = V_{zb}/c = [1 - (1 + a_w^2/2)/\gamma_b^2]^{1/2}$ is the average normalized axial velocity of a typical test electron, and γ_bmc^2 is the electron energy. For FEL operation with a cold, thin ($k_w^2x_b^2 \ll 1$) electron beam, the orbit of an individual beam electron corresponds to an untrapped orbit with energy $H = \gamma_bmc^2 > (1 + a_w^2)^{1/2}mc^2$.

The transverse field inhomogeneities in Eq. (4) can play an important role in altering

the electron motion when the wiggler field amplitude a_w and/or the normalized transverse displacement $k_w x$ become sufficiently large. We find that the electron motion undergoes a transition from regular motion to chaoticity, as a_w and/or the betatron oscillation amplitude are increased. In essence, the chaotic behavior originates from the coupling between the wiggle motion and the betatron oscillations, which is enhanced by increasing a_w and/or the betatron oscillation amplitude. Figure 1 shows the Poincaré surface-of-section plot in the phase plane (z, P_z) at $P_x = 0$ for beam energy $\gamma_b = 3.0$ and wiggler amplitude $a_w = 2.0$. In Fig. 1, the orbits corresponding to the untrapped orbits in the integrable limit ($k_w x = 0$) are obtained by integrating numerically the equations of motion derived from the Hamiltonian in Eq. (4) with the initial conditions $P_{x0} = 0$, $k_w z_0 = \pi/2$, and eleven choices of P_{z0} distributed uniformly in the range from $P_{z0} = mc$ to $P_{z0} = 2\ mc$. The condition $H(x_0, z_0, P_{x0}, P_{z0}) = \gamma_b mc^2$ or $\cosh(k_w x_0) = (\gamma_b^2 - P_z^2/m^2c^2 - 1)^{1/2}/a_w$ determines the initial normalized transverse displacement $k_w|x_0|$, which increases monotonically from 0 to 0.783 as P_{z0} decreases from $P_{z0} = (\gamma_b^2 - 1 - a_w^2)^{1/2}mc = 2\ mc$ to $P_{z0} = mc$. It is evident in Fig. 1(a) that the phase plane contains chaotic orbits as well as regular orbits [Kolmogorov-Arnol'd-Moser (KAM) tori[6]]. The chaotic orbits exhibit a sensitive dependence on the initial conditions and have positive Liapunov exponents. In Fig. 1(a), the main chaotic sea occupies a region of phase space with positive and negative axial momentum. Therefore, the chaotic orbits undergo a random walk axially. Typically, the reversal of the axial momentum in the chaotic orbits is found to occur within a few betatron oscillation periods. Moreover, the chaotic orbits exhibit *irregular* betatron oscillations with a maximum transverse displacement greater than the initial transverse displacement x_0. By contrast, the regular orbits undergo periodic or quasiperiodic betatron oscillations with the oscillation amplitude $x_m = x_0 \geq 0$. Figure 1(b) shows a close-up of Fig. 1(a) in the vicinity of the regular orbits with $P_z > mc$. In Fig. 1(b), the orbits with P_{z0} in the range $1.6\ mc \leq P_{z0} \leq 2.0\ mc$

are regular, corresponding to a normalized betatron oscillation amplitude in the range $0 \leq k_w x_0 \leq 0.57$. On the other hand, all of the orbits with $|P_z| < 1.6\ mc$ or $|k_w x| > 0.57$ are chaotic. In other words, for given γ_b and a_w, there exists a unique critical value of transverse displacement beyond which the electron orbits become chaotic. Therefore, we identify the onset of beam degradation due to chaotic effects to coincide with the onset of chaos in the electron orbits at the edge of the beam. With this definition, the parameter space $(\gamma_b, a_w, k_w x_b)$ can be divided into regular and chaotic regions for beam propagation. In the remainder of this article, we obtain an analytical estimate of the boundary between the regular and chaotic regions and compare the results with numerical simulations.

To determine the regular and chaotic regions, we expand Eq. (4) to order a_w^2/γ_0^2, where $a_w/\gamma_0 < 1$ is assumed. This yields

$$H \cong H_0 + H_\beta + H_c \ , \tag{5}$$

where

$$H_0 = \left[c^2 P_z^2 + \left(1 + \frac{a_w^2}{2}\right) m^2 c^4\right]^{1/2} \equiv \gamma_0 m c^2 \ , \tag{6}$$

$$H_\beta = \frac{1}{2\gamma_0 m}(P_x^2 + \gamma_0^2 m^2 \omega_\beta^2 x^2) \ , \tag{7}$$

$$H_c = -\frac{\gamma_0 m \omega_\beta^2}{4k_w^2}[\cosh(2k_w x) + 1]\cos(2k_w z) \ , \tag{8}$$

and $\omega_\beta = ck_w a_w/\sqrt{2}\gamma_0$ is the betatron oscillation frequency. In Eq. (5), the lowest-order Hamiltonian H_0 describes the average axial motion of the electron, the perturbation H_β describes the betatron oscillations, and the perturbation H_c describes the wiggle motion and the coupling between the wiggle motion and the betatron oscillations. It

follows from Eq. (7) that the solutions for the betatron oscillations can be expressed as $x(t) = x_m \cos(\omega_\beta t + \alpha)$ and $P_x(t) = -\gamma_0 m \omega_\beta x_m \sin(\omega_\beta t + \alpha)$, where x_m and α are the amplitude and phase of the oscillations, respectively. Substituting $x(t) = x_m \cos(\omega_\beta t + \alpha)$ into Eq. (8) and making use of the generating function for Bessel functions, it is readily shown that the condition for resonance between the wiggle motion and the nth harmonic of the betatron oscillations can be expressed as

$$n\omega_{\beta n} - ck_w\beta_{zn} = 0 \ , \qquad n = 0, \pm 1, \pm 2 \ \cdots \ . \tag{9}$$

Moreover, the width of the nth-order resonance W_n in P_z-space is given by

$$W_n = W_n(\gamma_n, a_w, k_w x_m) = \frac{2a_w\gamma_n mc}{(2+a_w^2)^{1/2}} \times \begin{cases} [1 + I_0(2k_w x_m)]^{1/2} \ , & (n = 0) \ , \\ [I_{2n}(2k_w x_m)]^{1/2} \ , & (n \neq 0) \ . \end{cases} \tag{10}$$

In Eqs. (9) and (10), $\omega_{\beta n} = ck_w a_w/\sqrt{2}\gamma_n$, $\gamma_n = [(n^2+1)a_w^2/2 + 1]^{1/2} < \gamma_{n+1}$, and $\beta_{zn} = P_{zn}/\gamma_n mc = [1 - \gamma_n^{-2}(1 + a_w^2/2)]^{1/2}$ is the betatron oscillation frequency, energy, and normalized axial velocity associated with the resonance of order n, respectively. Here, $I_n(x)$ is the modified Bessel function of the first kind of order n. Expressing Eq. (9) in the equivalent form $P_{zn} = \gamma_n\beta_{zn}mc = na_w mc/\sqrt{2}$, it follows that the momentum spacing between adjacent resonances is uniform and is given by $\Delta P_z = a_w mc/\sqrt{2}$. In the spirit of applying the Chirikov resonance-overlap criterion,[8] the electron orbits at the edge of the beam become chaotic when the total width of the resonances situated between $P_z = -P_{zm} = -(\gamma_b^2 - 1)^{1/2}mc$ and $P_z = +P_{zm}$ is greater than $2P_{zm}$. Here, $P_{zm} = (\gamma_b^2 - 1)^{1/2}mc$ is the maximum axial momentum of a beam electron with energy $H = \gamma_b mc^2$. Therefore, an approximate condition for the onset of chaos in beam propagation is given by

$$f(\gamma_b, a_w, k_w x_b) \equiv \sum_{n=-N}^{N} W_n(\gamma_n, a_w, k_w x_b) - 2(\gamma_b^2 - 1)^{1/2} mc = 0 \ , \qquad (11)$$

where $N = P_{zm}/\Delta P_z = [2(\gamma_b^2 - 1)]^{1/2}/a_w$ is the highest-order resonance in the range extending from $P_z = -P_{zm}$ to $P_z = +P_{zm}$. The function f defined in Eq. (11) is positive (negative) in the regular (chaotic) region of parameter space. Figure 2 shows plots of the regular and chaotic regions in the parameter space $(k_w x_b, a_w)$ for $\gamma_b = 3$ and 8. In Fig. 2, the dashed curves correspond to the analytical estimates obtained from Eq. (11), and the solid curves represent the corresponding numerical results obtained by generating Poincaré surface-of-section plots similar to Fig. 1. Despite the differences between the simulation results and analytical estimates of the boundary, the essential features are described well by our simple analytical model. Similar results can also be obtained for a realizable helical-wiggler field configuration.[9]

The implications of these results can be applied (for example) to the microwave FEL experiments by Orzechowski *et al.*,[4] which produce (with wiggler field taper) 1 GW of microwave power at 34.6 GHz. In the experiments,[4] an electron beam with energy 3.5 MeV and current 850 A is injected into a planar wiggler field with wiggler amplitude $B_w = 3.72$ kG and wiggler period $\lambda_w = 9.8$ cm. This corresponds to beam energy $\gamma_b \cong 8$ and dimensionless wiggler amplitude $a_w = eB_w\lambda_w/(2\pi mc^2) = 3.4$. Therefore, it follows from Fig. 2 that the normalized half-beam width $k_w x_b$ should not exceed unity in order to avoid chaoticity-induced beam degradation. As the wiggler field amplitude is increased to $B_w = 5$ kG ($a_w \cong 4.5$), say, the critical value of the normalized half-beam width $k_w x_b$ for the onset of chaos decreases to $k_w x_b \cong 0.7$.

To summarize, we have shown that the motion of an individual test electron in a low-density relativistic electron beam propagating through a realizable planar-wiggler magnetic field is nonintegrable, and exhibits chaotic behavior when the wiggler amplitude

is sufficiently large. The existence of chaotic electron orbits places limits on the wiggler field strength and the transverse beam dimension for beam propagation and free electron laser operation. An estimate of the boundary between the regular and chaotic regions in the parameter space $(\gamma_b, a_w, k_w x_b)$ was derived analytically and found to be in good qualitative agreement with the numerical simulations.

ACKNOWLEDGMENTS

This work was supported in part by the Department of Energy High Energy Physics Division, the Naval Research Laboratory Plasma Physics Division, and the Office of Naval Research.

REFERENCES

1. C.W. Roberson and P. Sprangle, Phys. Fluids **B1**, 3 (1989).
2. D.A.G. Deacon, L.R. Ellis, J.M.J. Madey, G.J. Ramian, H.A. Schwettman, and T.I. Smith, Phys. Rev. Lett. **38**, 892 (1977).
3. M. Billardon, P. Elleume, J.M. Ortega, C. Bazin, M. Bergher, V. Velgle, Y. Petroff, D.A.G. Deacon, K.E. Roberson, and J.M.J. Madey, Phys. Rev. Lett. **51**, 1652 (1983); R.W. Warren, B.E. Newman, and J.C. Goldstein, IEEE J. Quantum Electron. **21**, 882 (1985).
4. T.J. Orzechowski, B.R. Anderson, J.C. Clark, W.M. Fawley, A.C. Paul, D. Prosnitz, E.T. Scharlemann, S.M. Yarema, D.B. Hopkins, A.M. Sessler, and J.S. Wurtele, Phys. Rev. Lett. **57**, 2172 (1986).
5. C. Chen and R.C. Davidson, Phys. Fluids **B2**, 171 (1990).
6. A.J. Lichtenberg and M.A. Lieberman, *Regular and Stochastic Motion* (Springer-Verlag, New York, 1983).
7. E.T. Scharlemann, J. Appl. Phys. **58**, 2154 (1985).
8. B.V. Chirikov, Phys. Rep. **52**, 263 (1979).
9. C. Chen and R.C. Davidson, submitted for publication (1990).

FIGURE CAPTIONS

Fig. 1 Poincaré surface-of-section plots in the (z, P_z) plane generated from the Hamiltonian in Eq. (4) for $\gamma_b = 3.0$, $a_w = 2.0$, and $P_x = 0$. Plots corresponding to (a) the entire phase plane with $k_w z$ mod π, and (b) a close-up of Fig. 1(a) showing the vicinity of regular orbits with $P_z > mc$.

Fig. 2 Plots showing the regular and chaotic regions in the parameter space $(k_w x_b, a_w)$ for values of beam energy corresponding to $\gamma_b = 3$ and 8. The dashed lines are the analytical estimates obtained from Eq. (11), and the solid curves represent the corresponding simulation results.

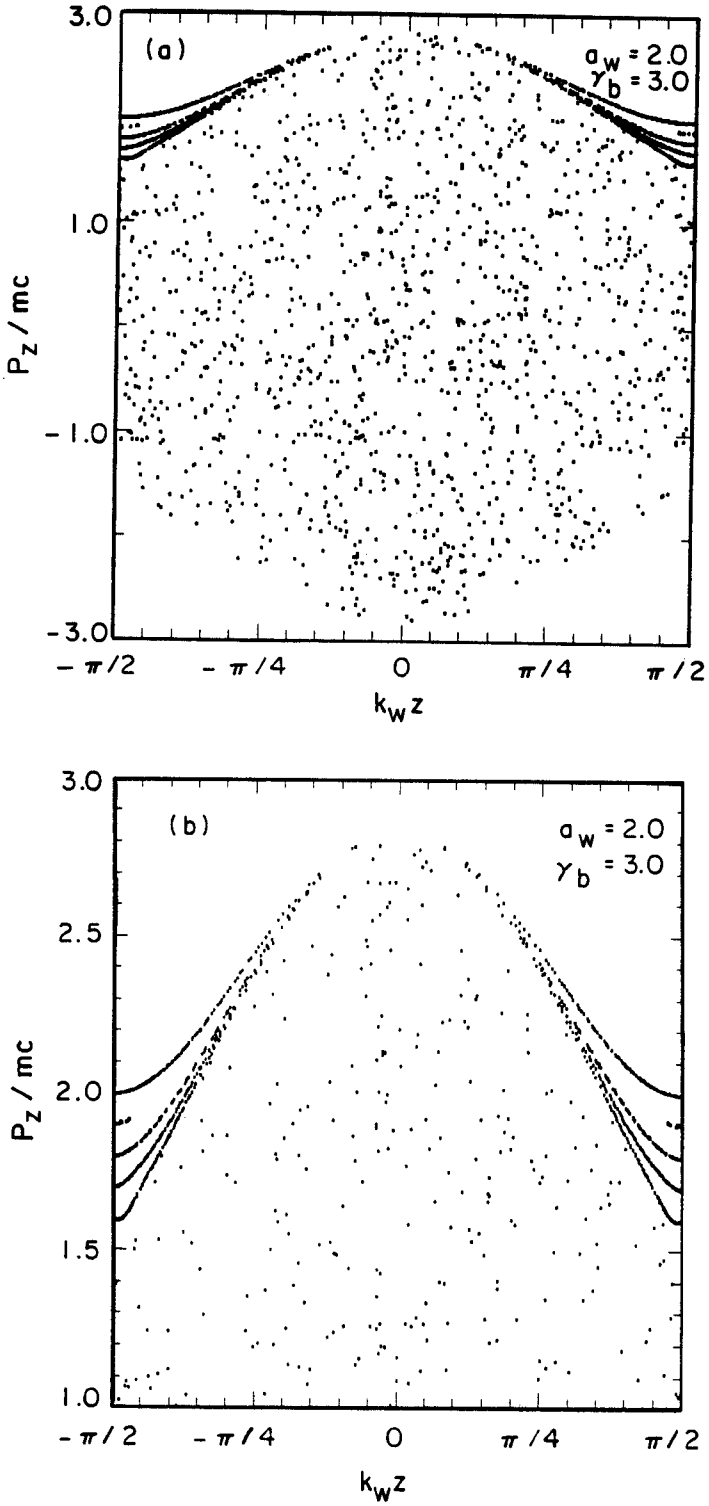
(a)
$a_w = 2.0$
$\gamma_b = 3.0$
3.0
1.0
-1.0
-3.0
P_z / mc
$-\pi/2$
$-\pi/4$
0
$\pi/4$
$\pi/2$
$k_w z$
(b)
$a_w = 2.0$
$\gamma_b = 3.0$
3.0
2.5
2.0
1.5
1.0
P_z / mc
$-\pi/2$
$-\pi/4$
0
$\pi/4$
$\pi/2$
$k_w z$

Figure 1

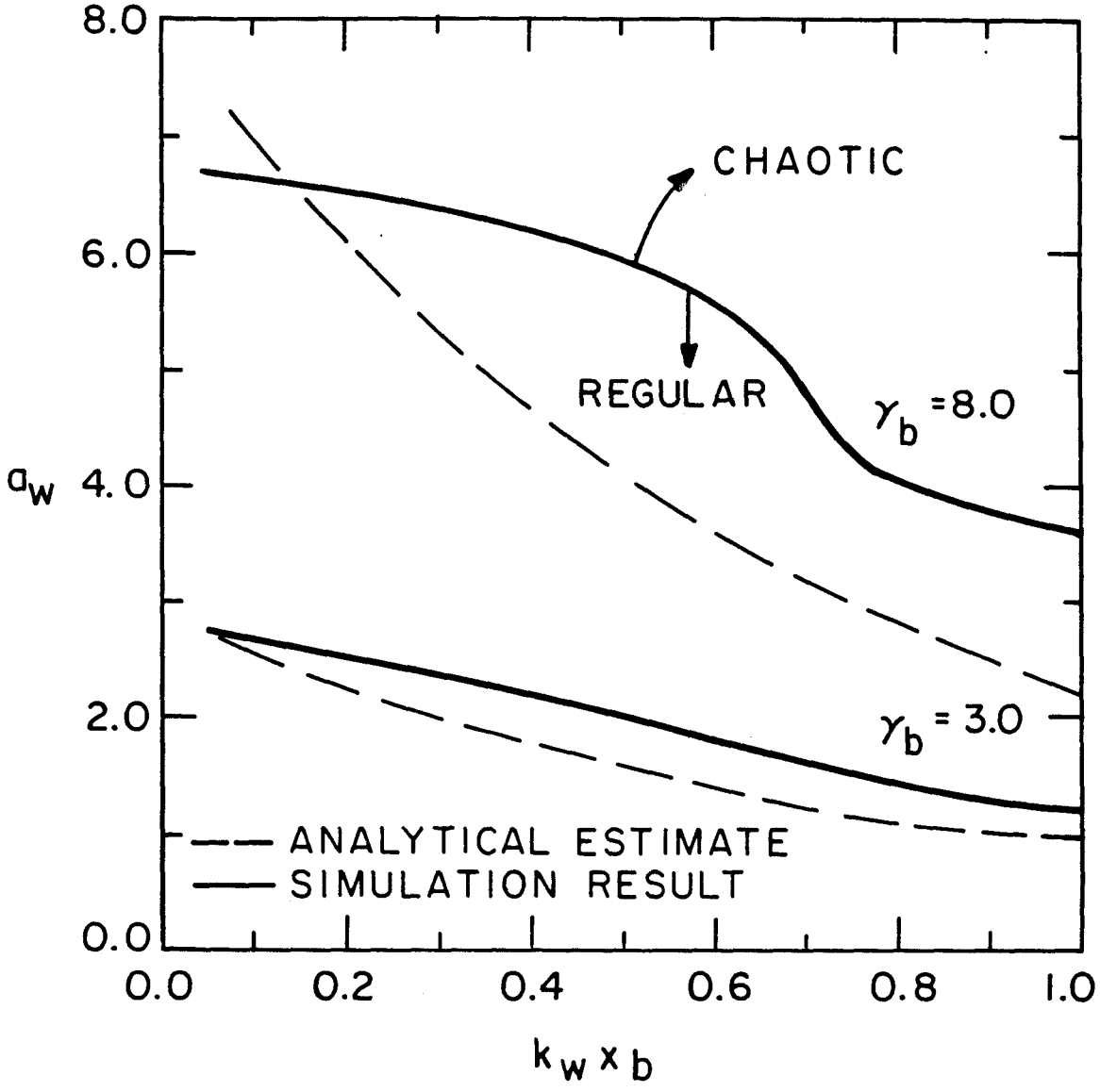
8.0
6.0
4.0
2.0
0.0
a_w
CHAOTIC
REGULAR
γ_b =8.0
γ_b = 3.0
ANALYTICAL ESTIMATE
SIMULATION RESULT
0.0
0.2
0.4
0.6
0.8
1.0
$k_w x_b$

Figure 2